PERGAMON

Computerized Medical Imaging and Graphics 25 (2001) 405–415

Computerized Medical Imaging and Graphics

www.elsevier.com/locate/compmedimag

Growing-cube isosurface extraction algorithm for medical volume data

T.-Y. Lee*, C.-H. Lin

Visual System Laboratory (VSL), Department of Computer Science and Information Engineering, National Cheng Kung University, Tainan, Taiwan, Republic of China

Received 18 July 2000; accepted 1 December 2000

Abstract

In medical applications, three-dimensional volume data such as CT and MRI are gathered from medical-imaging devices. Marching cube (MC) algorithm is a common routine to extract isosurfaces from volume data. The MC algorithm generates the massive number of triangles to represent an isosurface. It is difficult to render this amount of triangles in real-time on general workstations. In this paper, we present a growing-cube algorithm to reduce the number of triangles generated by the MC algorithm. Growing-cube algorithm uses a surface tracker to avoid exhaustive searching isosurfaces cell-by-cell and, therefore, it saves computation time. During surface tracking, the growing-cube algorithm adaptively merges surfaces contained in the tracked cells to reduce the number of triangles. Surfaces are merged as long as the error is within user-specified error thresholds. Therefore, the proposed algorithm can generate a variable resolution of isosurfaces according to these error parameters.

Keywords: Marching-cube; Growing-cube; Surface tracking and merging; Meta-surface; Surface triangulation

1. Introduction

In medical applications, major sources of three-dimensional volume data are gathered from medical-imaging devices such as CT, MRI and PET scanners. Generating polygons to approximate surfaces of organs from 3D volume data has been widely used by clinicians to visualize, manipulate and measure three-dimensional internal structures of patients. Many algorithms [1–4] have been proposed to generate isosurfaces from volume data. Among them, the marching cube (MC) algorithm [4] has been used as a standard isosurface generation algorithm. Using the MC method, the number of triangles generated per cell varies from one to five. Therefore, for example, for given a $512 \times 512 \times 100$ medical CT data, the MC algorithm potentially produces the number of triangles varying from 500 to 2000 K. This sheer amount of triangles is still prohibitive to achieving a real-time rendering on most workstations. In the past, much effort has been made to reduce this amount. The solutions proposed can be roughly classified into two categories. The first class produces triangles using the MC algorithm, and then employs polygon simplification methods to reduce the number of triangles [2,5,6]. In contrast, the second class exploits adaptive techniques [1,7–10] to reshape the cube size or to down-sample the volume data set where the isosurface is mostly flat. In this paper, the proposed method, called growing-cube method, does not reshape nor down-samples volume cells, but it adaptively generates varying-size surfaces.

Other issues, such as ambiguity problem in the method of approximating the surface [11–14], the redundant polygon generation problem [15], and computational speed improvement [8,10,16] have attracted many researchers to work on them. In this paper, the proposed method can save the number of triangles as well as save computational timings. In some situation, not all components of the isosurface are connected. Bajaj et al. [20] and Westermann et al. [21] resolved this contour following problem. Growing-cube method fails if the isosurface has more than a connected component, since traversal starts from a single seed. Actually, experience with visualizing our medical applications has shown that most datasets have only a connected component. If required, to resolve this situation, multiple-seeds are allowed to interactively insert to extract all components of the isosurface.

The remainder of this paper is organized as follow. In the next section, we will review the most related prior work. Section 3 will introduce each step of the proposed method in details. The experimental results for artificial data sets and medical volume data are described and discussed in Section 4. Finally, we give the summary of this paper in Section 5.

* Corresponding author. Tel.: +886-6-2757575; fax: +886-6-2747076.
E-mail address: tonylee@mail.ncku.edu.tw (T.-Y. Lee).

0895-6111/01/$ - see front matter
PII: S0895-6111(00)00084-7

2. Previous work

Van Gelder et al. [16] employed an Octree data structure to reduce the number of cubes traversed, and thus they improved the MC's computational efficiency. However, this approach does not reduce the number of triangles generated by the MC algorithm. In contrast, Ning et al. [8] attempted to use an Octree to assist in decimating the number of triangles. However, this algorithm is not very efficient in computation. Shu et al. [7] proposed an adaptive marching cube (AMC) algorithm to reduce the number of triangles representing the surface. This method is limited to data sets of resolutions of the power of two. The initial cubes are recursively subdivided into eight sub-cubes, if the approximating surface has high curvature. This approach has potential to miss small objects inside the cube. Independently, Muller et al. [1] proposed a similar approach termed as splitting-box algorithm. Li et al. [15] improved MC algorithm in two ways. First, this method simply uses the middle point as the triangle vertices between two adjacent sample points. Second, it detects the redundant triangles and eliminates them. Similarly, Montani et al. [17] proposed a discretized MC method where the edge intersections are approximated by edge midpoints. Furthermore, the discretized MC also builds superfaces and simplifies them. Yagel et al. [9] proposed an Octree-based strategy to decimate the number of triangles of MC. Like Ref. [7], this method requires additional stage to deal with crack patching problem. However, this method is better than Ref. [7], since its crack patching does not introduce new triangles. Park et al. [10] presented a vertex-merging algorithm that merges the vertices of triangles generated by the MC algorithm at a surface generation step. It is a bottom-to-up approach, and hence, it avoids cracks and missing small objects in cube. In this approach, it still exhaustively searches all cells.

3. Growing-cube algorithm

The growing-cube algorithm consists of three components as shown in Fig. 1. The surface tracking searches each cell through which the isosurface passes instead of exhaustive searching in the MC algorithm. The connected surface contained in a searched cell can be merged (or grown) into a large connected surface called meta-surface. The surface tracking and meta-surface merging are executed at the same time. A meta-surface can grow into an arbitrarily large surface as long as the growing condition is met. Once a meta-surface cannot grow, we triangulate it and then start another new meta-surface growing if necessary. Each component of algorithm is explained in detail below.

3.1. Surface tracking

The MC algorithm generates triangles cell-by-cell to approximate isosurfaces. The values of grid points and

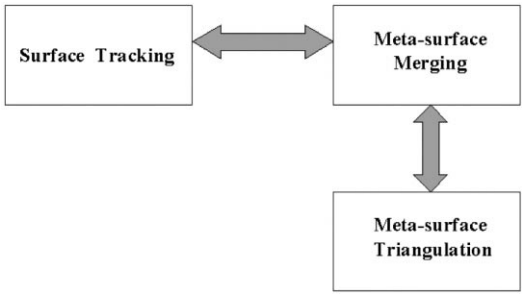

Fig. 1. Three components in the proposed Growing-cube algorithm.

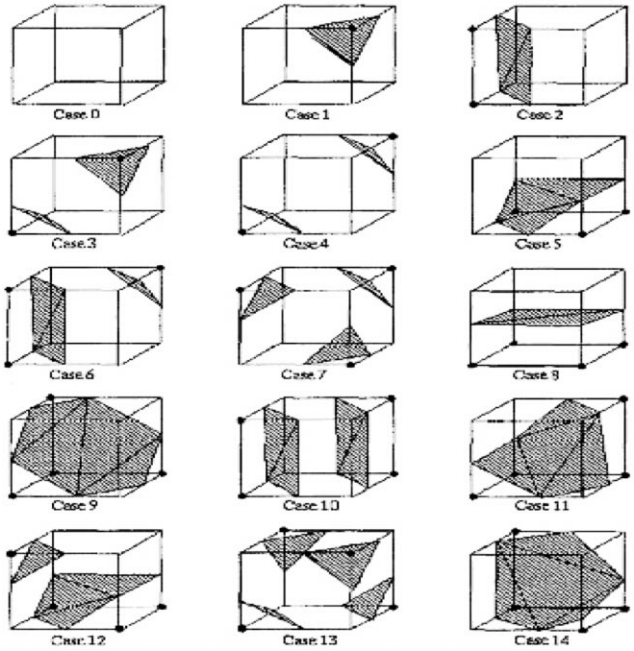

Fig. 2. Topologically different configurations of the MC algorithm.

linear interpretation are used to determine where the isosurface intersects an edge of a voxel. In total, there are only 15 topologically different configurations, as shown in Fig. 2. Like Ref. [9], we employ a surface tracker to identify each cell through which the isosurface passes. The user specifies a seed cell that is not an ambiguous configuration of the MC algorithm and then the surface tracker starts searching seed's neighboring cells. For each cell, at most, there are six tracking directions. Among 15 cases, those cases 0, 1, 2, 3, 5 and 8 do not need to track six neighboring cells. Yagel et al. [9] pointed that these six cases account for 90% of the cases encountered in extracting an isosurface in their applications. Therefore, the tracking approach leads to more saving in computation. To speed up surface tracking, a look-up table is created and is used to guide which cells to visit from a given cell. To create this table, we label each edge e_i [as shown in Fig. 3(a)] and six tracking directions [as shown in Fig. 3 (b)] for a given cell. This look-up table is shown in Fig. 4. For example, if a cell is identified as case 1 of the MC configurations, this cell has three

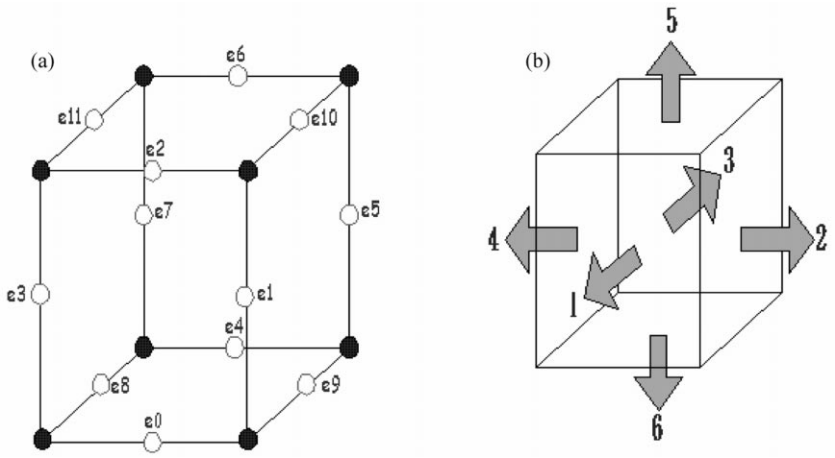

Fig. 3. Edge and direction labeling.

intersected edges, (e_1, e_2), (e_1, e_{10}) and (e_2, e_{10}). Then, we use these three edge pairs as indexes to retrieve tracking directions from the look-up table. Like (e_1, e_2), table $[e_1, e_2] = 1$ says the current cell needs to track that cell in the direction of '1'.

3.2. Meta-surface growing

The user specifies a seed cell that is not an ambiguous case of MC method and contains connected triangular surfaces like cases 2, 5, 8, 9, 11 and 14. Then, the seed meta-surface attempts to grow into an arbitrary large one by merging neighboring meta-surfaces contained in neighboring cells. Recursively, this meta-surface growth toward tracking directions continues until that the growing criteria are violated. Then, this violated meta-surface can be a new seed to start another meta-surface growing. During growing, the normal of the meta-surface is always used and is computed by finding the normal of the best-fit plane for all triangular patches contained in the cell. Fig. 5 assumes that a growing meta-surface *GM* whose normal is (N_x, N_y, N_z), attempts to merge another meta-surface F whose normal is (F_x, F_y, F_z) contained in a tracked cell. The following criteria must be satisfied for above meta-surface growth. Once merge is successful, we compute a new (N_x, N_y, N_z) [1] to represent this new and larger meta-surface.

	e_0	e_1	e_2	e_3	e_4	e_5	e_6	e_7	e_8	e_9	e_{10}	e_{11}
e_0	*	1	1	1	6	*	*	*	6	6	*	*
e_1	1	*	1	1	*	2	*	*	*	2	2	*
e_2	1	1	*	1	*	*	5	*	*	*	5	5
e_3	1	1	1	*	*	*	*	4	4	*	*	4
e_4	6	*	*	*	*	3	3	3	6	6	*	*
e_5	*	2	*	*	3	*	3	3	*	2	2	*
e_6	*	*	5	*	3	3	*	3	*	*	5	5
e_7	*	*	*	4	3	3	3	*	4	*	*	4
e_8	6	*	*	4	6	*	*	4	*	6	*	4
e_9	6	2	*	*	6	2	*	*	6	*	2	*
e_{10}	*	2	5	*	*	2	5	*	*	2	*	5
e_{11}	*	*	5	4	*	*	5	4	4	*	5	*

Fig. 4. Look-up table used for surface tracking. Non-existing direction is marked by '*'.

1. The angle between (N_x, N_y, N_z) and (F_x, F_y, F_z) must be less than a threshold, θ_N.
2. The shortest distance from each triangular patch of F to *GM* must be less than a selected threshold, *dist*. The above two conditions guarantee two faces are flat enough.
3. We also require the normal of each vertex contained in F must be similar to (N_x, N_y, N_z). In other words, the angle between normals must be less than a threshold denoted as θ_V. The shading effect is related to vertex normals. This condition guarantee there is no too much difference in shading effect between F and *GM*. In the proposed approach, we use a meta-surface F to approximate the connected triangular patches. In some case such as case 5, these connected triangular patches are not very flat. It is not correct to use a meta-surface F to represent them. This condition avoids this error happening.

[1] Later in this section, we actually use the normal of a seed-meta-surface instead.

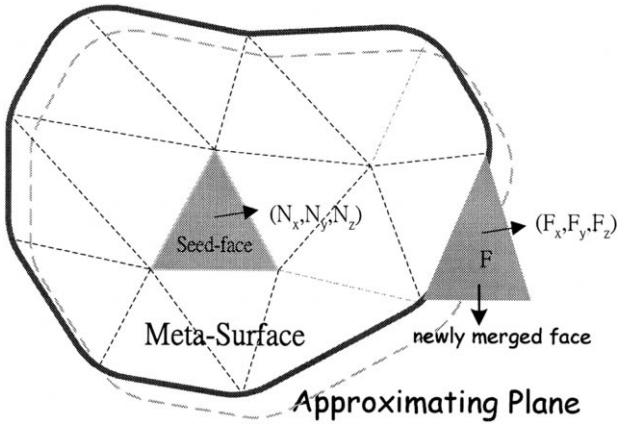

Fig. 5. ***Meta-surface*** growing.

4. A meta-surface F (i.e. case 1, 2, 5, 8, 9, 11 or 14) must be connected and then be considered to merge with GM. Disconnected cases are isolated from the meta-face growing and their triangular patches are output directly.
5. Both meta-faces F and GM cannot fold over on their approximating plane. Later, we perform surface triangulation in two-dimension rather than three-dimension. We need to compute orthogonal projection of vertices of F on the plane containing GM. If there is some fold-over occurring, it fails to triangulate the merged surface. This condition is used to guarantee the correctness of meta-surface triangulation in the proposed algorithm.

Merging can start if all of the above five conditions are met. When two faces are allowed to merge, the merging is simply done by eliminating the shared edge as shown in Fig. 6. The meta-surface maintains the boundary edges and internal edges are removed. Later, the surface triangulation is employed to adaptively add internal edges into the meta-face. There is an implementation issue about finding the approximated plane. One possible solution is to find the best approximating plane to contain both meta-surfaces GM and F for each meta-surface merging. Once a new face is merged, and then a new approximating plane is computed. Generally, this computational time grows linearly with the number of faces being merged. Each surface included in the GM and F must be checked against the non-fold-over rule (condition 5). Assume that there are n faces merged in final, the merging is computed in O (n^2) time. Therefore, this solution seems not very efficient in computation. To reduce this cost, we alternatively use the plane containing the seed face rather than compute a newly approximating plane every-time. From our viewpoint, if the faces can merge with a given seed face, these merged faces should be almost on the same plane containing the seed face. Otherwise, they should not merge. Therefore, we use this solution instead. Now, we do not need to compute an approximating plane whenever a new face is merged. Furthermore, we do not need to re-check all merged faces against the no-fold-over rule every time. In this simplified implementation, only the newly meta-surface F is required to be verified. Therefore, in total, this cost can be reduced from O (n^2) to O (n).

Now, let us present the growing-cube algorithm and its pseudo-code is outlined in Fig. 7. In this implementation, we maintain two queues, namely ***DirQueue*** and ***SeedQueue***. For the ***DirQueue***, it records the possible tracking directions for the current meta-surface. In case that the current cell cannot merge, this cell is inserted in the ***SeedQueue*** instead. Later, once this cell is pop up from the ***SeedQueue***, and then it potentially starts a new meta-surface growing. In this pseudo code, a 3D flag array (i.e. is initialized flag = 0) exactly the size of the 3D dataset is used. The *flag* value of the cell indicates this cell whether it has been tracked (flag = 1), or the cell was in the ***DirQueue*** (flag = 2) or that was in the ***SeedQueue*** (flag = 3). Therefore, this 3D flag array avoids cells being tracked and queued more than once. In the inner loop, if the current F satisfies the growing criteria, we perform face merging. Otherwise, we insert this cell into the ***SeedQueue***, and later this cell can potentially start a new meta-surface growing. Whenever the current meta-surface accomplishes its growth (i.e. leave the inner loop), we start triangulating the current meta-surface and output its triangular surfaces. Then, we pop up a new cell from the ***SeedQueue*** and enter the inner loop again. The above process will not finish until both the ***DirQueue*** and the ***SeedQueue*** are empty. Note that once ambiguous cases take place and we employ [22] to solve this ambiguity.

Fig. 8 is an example to show that the proposed algorithm

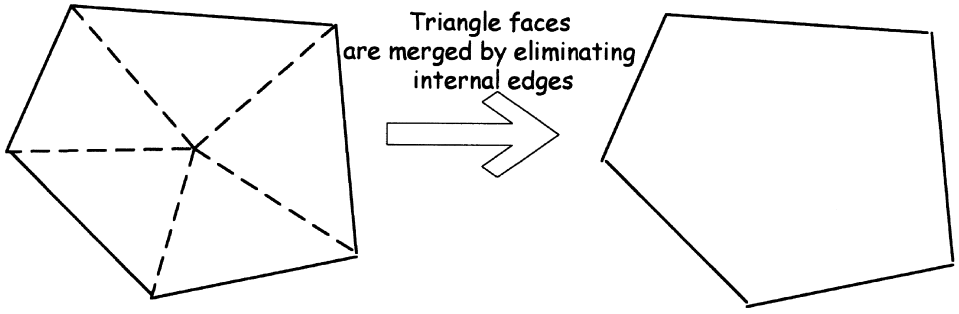

Fig. 6. Face merging.

Algorithm *Growing-cube*

Input: a seed cell (*i,j,k*) that contains an unambiguous configuration of MC algorithm and its triangular patches are connected;

Output: triangular surfaces

Begin

For all tracking directions of a seed cell (*i,j,k*) using the proposed ***surface-tracker***

Insert cells located on tracking directions into the ***DirQueue***;

While (***SeedQueue*** != NULL) {

While (***DirQueue***!= NULL) {

Remove a new cell termed as (*i,j,k*), from the ***DirQueue***;

Find its MC configuration and determine if it is qualified as a meta-surface *F* or not (i.e., must be connected)

If cell (*i,j,k*) is an ambiguous case , we solve its ambiguity by the method in [22] and directly output its triangular patches. Then, we insert cells located on tracking direction of cell (*i,j,k*) into SeedQueue and set flag of cell (i,j,k) to be 1;

Else If *F* is a disconnected case of the MC algorithm, we directly output its triangular surfaces and insert each tracking direction into SeedQueue and set flag of (i,j.k) to be 1;

Else If a qualified *F* exists and all growing criteria are met,

{

1. The meta-surface *F* merges with the current ***meta-surface*** *GM*
2. Set the flag of (i,j,k) to be 1;
3. For each tracking direction of cell (i,j,k), a neighboring cell say (*i',j',k'*)

If cell (*i',j',k'*) has not been tracked (*i.e*, $flag = 0$)

a. insert (*i',j',k'*) in the ***DirQueue***

b. set flag of (*i',j',k'*) to be 2;

//* it avoids (*i',j',k'*) being tracked more than once;

}

Else If the cell (*i,j,k*) (*i.e.*, $flag \neq 3$)is not in the ***SeedQueue***;

// * cell (i,j,k) does not meet the growing criteria

{

insert cell (*i,j,k*) in the ***SeedQueue***;

set *flag* of the cell (*i,j,k*) to be 3

// ** to avoid being inserted more than once**/

}

}

Triangulate the current ***Meta-surface***

Output triangular surfaces;

}

Fig. 7. Growing-cube algorithm.

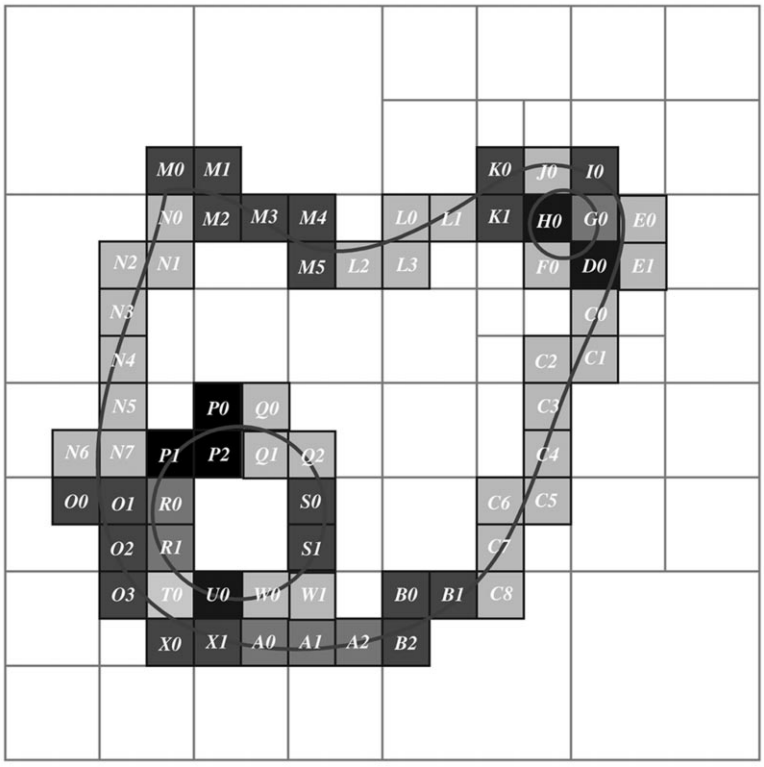

Fig. 8. An example of isosurface extraction.

potentially performs better than an Octree-based approach [9]. In this figure, each meta-surface is labeled by a distinct alphabet. The meta-surface C consists of several small meta-surfaces contained in nine cells numbered by C_0, C_1… and C_8, respectively. These nine cells can merge by means of the proposed method. In contrast, the Octree-based approach generates four smaller meta-surfaces, (C_0, C_1), C_2, (C_3, C_4, C_5, C_6, C_7) and C_8, respectively. In this example, there are several similar cases such as meta-surfaces M and N. Our comment is that the Octree is a good data structure to organize merging process [9], but also limits the freedom of merging. From this respect, the proposed algorithm has an advantage over [9].

3.3. Meta-surface triangulation

We triangulate meta-surfaces in 2D rather than in 3D and describe this process as follows. First, we project all boundary vertices of a meta-surface on the approximating plane. Here, the plane of a seed meta-surface is used as the approximating plane. Next, we add internal vertices into the meta-surface to form several triangular meshes. To find a suitable triangulation method is essential at this stage. In particular, this triangulation must handle hole problem. For example, in Fig. 9, there are several meta-surfaces denoted as S_1, S_2,… and S_5 and these meta-surfaces are surrounded by a single neighboring meta-surface S_0. In this situation, while triangulating this meta-face S_0, we create a hole. To solve this problem, we employ [18] to triangulate the meta-surface. This method was extended [18] from Seidel's fast polygon triangulation method [19] to handle hole problem.

To directly triangulate the meta-face might be not the best implementation. Fig. 10(a) shows an example of a typical meta-surface after merging. In this example, there are many gear-tooth-like edges appearing in the boundary of the meta-surface. These gear-tooth-like edges lead to more triangular surfaces. To avoid this, we use a simple poly-line approximation to best fit these edges and thus to reduce the number of gear-teeth as shown in Fig. 10(b). For the poly-line approximation, we need to set up a distance error, ϵ. If the distance between a gear-tooth and an approximating poly-line is within the distance error, this gear-tooth can be eliminated. After this simplification process, we proceed to triangulate the meta-surface. Considering all cases of MC algorithm, those cases 3, 4, 6, 7, 10, 12 and 13 are with

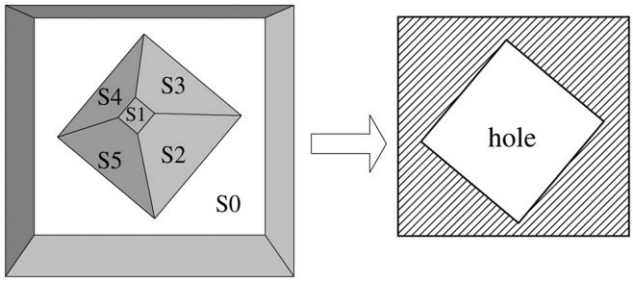

Fig. 9. Hole occurs in surface triangulation.

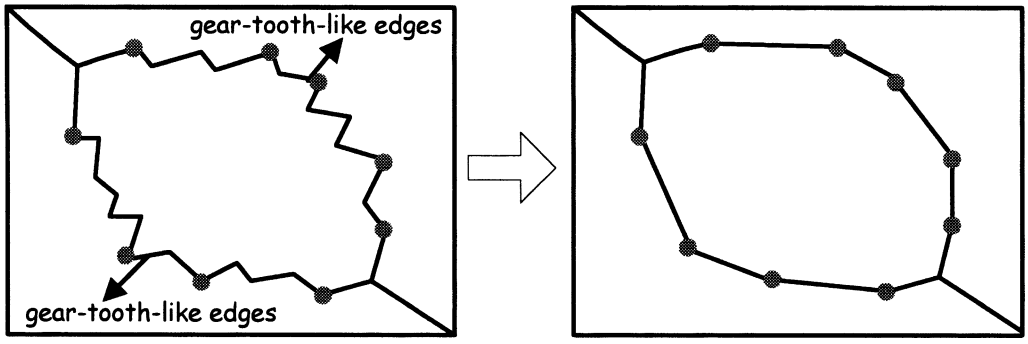

Fig. 10. (a) Gear-tooth-like boundary of meta-surface; (b) boundary simplification.

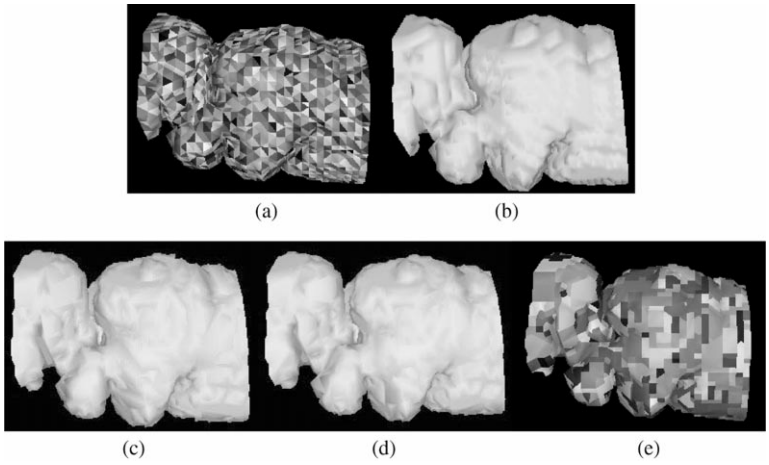

Fig. 11. CT Colon: (a) the original MC triangular mesh; (b) MC rendering results; (c) Growing-cube, 78% decimation; (d) Growing-cube, 86% decimation; and (e) the ***meta-surface*** of (d) case, where each meta-surface is shaded with different colors.

disjointed triangular surfaces. Since these triangular surfaces are located at a given cell, the distance between two surfaces is very small. If this distance is smaller than the threshold ϵ, the proposed algorithm potentially merges two disjointed surfaces by mistake during this border simplification. For example, in Fig. 8, in cell T_0, there are two disjointed iso-surface contours. If these two surfaces are merged incorrectly, it becomes a connected isosurface. This is another reason why we require that a given cell can be merged if it is a connected surface configuration of the MC algorithm.

4. Results and discussions

To evaluate the proposed algorithm, we also implemented the original MC algorithm and executed both algorithms on a Pentium II-300 personal computer.[2] The following four datasets were used in our evaluation: (1) $256 \times 256 \times 30$ Colon CT dataset (Fig. 11), (2) $128 \times 128 \times 56$ CT Head dataset (Fig. 12), (3) $128 \times 128 \times 128$ artificial Stomach dataset (Fig. 13) and $16 \times 16 \times 16$ volumetric Cube dataset (Fig. 14). Table 1 compares the execution time of the surface tracker and the original MC algorithm. As shown in this table, the surface tracker always performs faster than the MC algorithm, and thus the proposed method gains computational saving. Experimental results show that the computational saving might not exactly increase with increasing resolution of datasets. In fact, it depends on the ratio of the number of non-empty cells over the size of volume data. To verify this observation, we also show the ratio information in Table 1. Among these four datasets, the Colon dataset performs the best due to

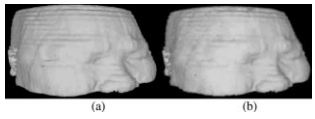

Fig. 12. CT head: (a) the original MC rendered results; and (b)at 80% decimating rate, rendered results using Growing-cube.

[2] We do not intend to compare the proposed method with the MC method, since it may be not appropriate. However, it is difficult to exactly re-implement other improved MC methods and to evaluate performance comparison on different platforms. Therefore, like previous studies [9,10], we use MC method as a golden standard to evaluate the proposed method.

Table 1
Computational saving of the surface tracker

Dataset method	Execution time (s)			
	Colon (256 × 256 × 30)	Head (128 × 128 × 56)	Stomach (128 × 128 × 128)	Cube (16 × 16 × 16)
MC	3.55	12.34	10.01	0.11
Tracking	0.68	6.46	6.74	0.06
Saving (%)	80.8	47.7	32.26	46.5
Ratio (%)	5.16	12.91	20.5	11.28

Table 2
Various thresholds used in Colon (Fig. 11), CT head (Fig. 12), Stomach (Fig. 13) and Cube (Fig. 14) datasets

	Plane normal (θ_N)	Vertex normal (θ_V)	*Dist* (pixel)
Fig. 11(c)	11°	15°	0.6
Fig. 11(d)	15°	20°	1.6
Fig. 12(b)	10°	15°	1.1
Fig. 13(b)	18°	15°	0.4
Fig. 13(c)	25°	30°	0.5
Fig. 13(d)	35°	35°	0.5
Fig. 13(e)	35°	35°	1.2
Fig. 14(c)	1°	30°	0.1

the lowest ratio of no-empty cells. The isosurfaces extracted by both MC and surface tracker are identical for each dataset.

Figs. 11–14 show experimental results for Colon, CT head, Stomach and Cube datasets. In these figures, we represent different meta-surfaces with different colors to observe the growing results of the meta-surface. Table 2 shows various thresholds used in these four experiments. These thresholds are defined in Section 3.2 (growing criteria). Table 3 shows the timing breakdown of these experimental results. In this table, the time taken in building meta-surface includes both surface-tracking and growing timings. Compared with the original MC algorithm, the total cost of the proposed method is increased by about 36% for colon, 65% for CT head, 26% for Stomach and 9% for Cube dataset, respectively. However, we can achieve very high decimation rates such as 86% in colon, 79% in CT head, 69% in Stomach and 94% in Cube. Rendered results of Stomach dataset, for example, for non-decimation [Fig. 13(f)] and decimation models [Fig. 13(g)–(j)] are very similar in the visual quality. However, the number of triangles decimated is very high up to 69%. In Table 3, we also show the number of meta-surface and triangles generated. These numbers show a consistent trend: as specifying larger thresholds in Table 2, we can generate less number of

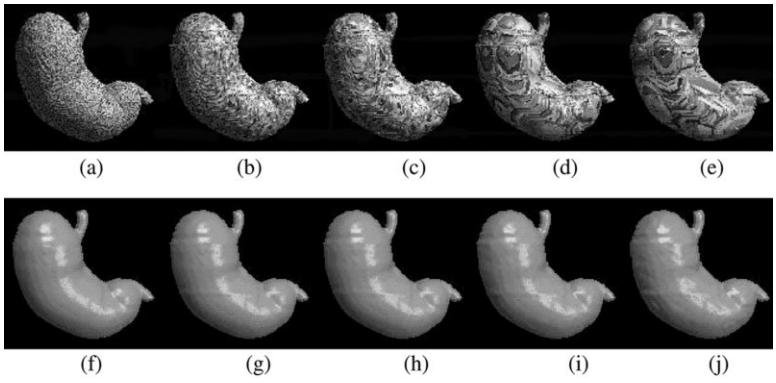

Fig. 13. Stomach: (a) the original MC triangular mesh; (b)–(f) by the Growing-cube method at 49, 54, 61 and 68% decimating rates, respective and (f)–(j) the rendered results of (a)–(e), respectively.

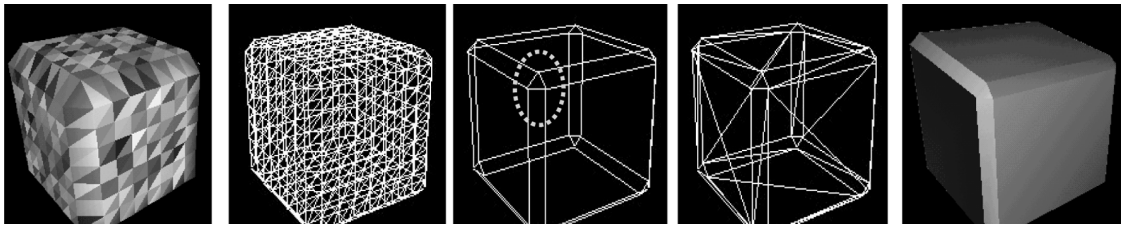

Fig. 14. Cube: (a) the original MC triangular mesh; (b) MC triangular wire-frame, (c) and (d) are wire-frames of meta-surface and triangular mesh at 94% decimating rate using Growing-cube method; and (e) shows the same meta-surface but encoded in different colors.

Table 3
Timing breakdown of experimental results for Colon (Fig. 11), CT head (Fig. 12), Stomach (Fig. 13) and Cube (Fig. 14) datasets

	Execution time(s)					
	Building meta-surface	Triangulation	Total time	Number of meta-surfaces	Number of triangles	Decimation rate (%)
Fig. 11(b)	–	–	3.55	–	23358	–
Fig. 11(c)	3.42	1.82	5.24	482	5113	78.11
Fig. 11(d)	3.13	1.73	4.86	282	3323	85.78
Fig. 12(a)	–	–	12.34	–	96548	–
Fig. 12(b)	11.21	9.21	20.42	9566	20124	79.51
Fig. 13(a)	–	–	32.32	–	72652	–
Fig. 13(b)	29.12	15.01	44.13	11146	36332	49.99
Fig. 13(c)	28.01	14.87	42.88	7933	32704	54.98
Fig. 13(d)	27.45	14.12	41.57	6446	27894	61.60
Fig. 13(e)	26.85	13.85	40.70	5197	22613	68.87
Fig. 14(a)	–	–	0.11	–	764	–
Fig. 14(d)	0.10	0.02	0.12	26	44	94.25

meta-surface and triangles. For example, when the larger thresholds are used for colon dataset [Fig. 11 (c) and (d)], the decimating rate is obviously increased from 78 to 86%. Other datasets such as CT head [Fig. 12(b)] and Stomach [Fig. 13(g)–(j)], have the same trend in decimating rate.

To demonstrate the ability of decimation, we use a volumetric Cube dataset to evaluate the proposed method, too. Fig. 14 shows different representations of the Cube dataset. In this example, each face of cube is successfully grown into a single meta-surface, and each meta-surface is triangulated into two triangular surfaces. However, for vertices on or near to the edges [as indicated by a circle in Fig. 14(c)], because of large difference in θ_V., we need to increase θ_V. up to 30° in our experiments. For the non-edge vertices, we just need to set a smaller θ_N., say 1°. Then, we can significantly decimate them in this example.

Next, we would like to measure accuracy of surface representations generated by the proposed method. For this purpose, we compare the difference in term of a voxel width between surfaces generated by the Growing-cube (GC) and the original MC algorithm. For above four experiments, Fig. 15(I)–(IV) visualize this measurement using color code and this color-coded visualization can help us understand to qualify the error introduced by the proposed method in global fashion. In each color bar, the lower (red) means the higher error introduced and the higher (blue) means the lower error generated. In each figure, we also indicate the average error in term of the width of a voxel. From these figures and their average errors, we can see the Growing-cube algorithm can significantly decimate the number of triangles as well as can preserve good quality of surfaces. For example, in Fig. 15(I), as we decimate 86% of triangles in the original Colon triangles, the average error introduced by the Growing-cube (GC) is 0.185 voxel width. Among these four examples, the Cube case performs the best. The average error is zero, so the color code (IV) of Cube is all blue.

5. Summary

In this paper, we present a Growing-cube algorithm to improve implementation of the MC algorithm. The proposed approach includes an adaptive decimation technique to generate various resolutions of models according to user-specified thresholds. It tracks connected surfaces instead of exhaustive searching iso-surfaces cell-by-cell. Therefore, it saves computation timing in identifying iso-surfaces. For our four test datasets, this saving varies from 30 to 80%. We conclude this gain is in inverse proportion to the ratio of non-empty cells over the entire volume cells. The lower ratio it is, the more efficiency it gains. The complete isosurface generated by the surface tracker is identical to that of MC method. Additionally, the proposed algorithm does not require additional data structure like Octree to speed up traversing cells [16] or to decimate triangular mesh [8,9]. From our experimental results, we find that the visual quality of rendering for both non-decimated and decimated models is nearly indistinguishable. For example, see rendered results for Stomach dataset. Therefore, compared with that of the MC method, we can use decimated models instead in our applications to save rendering time, too. Additionally, the total execution cost of the proposed algorithm is increased ranging from 9 to 65 % for all experiments, while we achieve decimating rate varying from 78 to 94%. From this respect, it is quite cost-effective. Some work can be done in near future. For example, in the current implementation, the proposed method grows face in a greedy manner. The greedy approach might be a sub-optimal method only. In future, we will develop a strategy to optimize our growing stage.

Acknowledgements

This work is supported in part by NSC-89-2218-E-006-028, National Science Council, Taiwan, Republic of China.

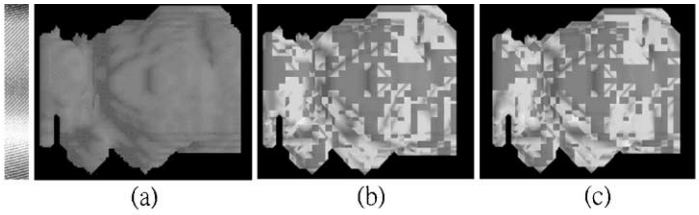

(I) Average error for Colon example in Figure 11

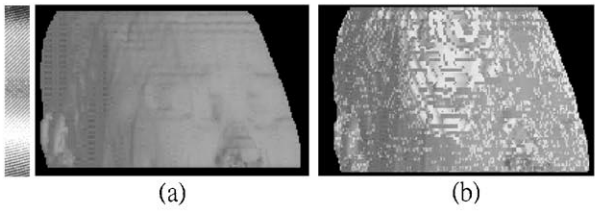

(II) Average error for CT Head example in Figure 12

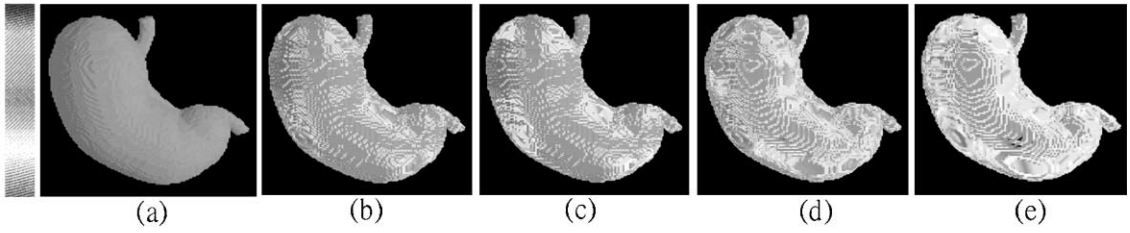

(III) Average error for Stomach example in Figure 13

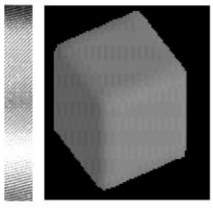

(IV) There is no error introduced by GC for Cube example (e) in Figure 14

Fig. 15. The visualization of error introduced by the Growing-cube (GC) method using color code for four experiments. In these figures, we also indicate the average error introduced in terms of the width of a voxel. For colour illustration, please see http://couger.csie.ncku.edu.tw/~vr/G_cube.html

References

[1] Muller M, Stark M. Adaptive generation of surfaces in volume data. The Visual Computer 1993;9:182–99.
[2] Schroeder WJ, Zarge J, Loresen WE. Decimation of triangle meshes. Computer Graphics 1992;26:65–70.
[3] Wyvill G, McPheeters C, Wyvill B. Data structure for soft objects. The Visual Computer 1986;2:227–34.
[4] Lorensen W, Cline H. Marching cubes: a high resolution 3-D surface construction algorithm. Computer Graphics 1987;21:163–169.
[5] Hoppe H, DeRose T, Duchamp T. Mesh Optimization. Computer Graphics Proceedings, Annual Conference Series, 1993. p. 19–26.
[6] Turk G. Re-tiling polygon surfaces. Computer Graphics 1992;26:55–64.
[7] Monhan S, Shu KR, Zhou C. Adaptive marching cubes. The Visual Computer 1995;11:202–17.
[8] Ning P, Hesselink L. Octree pruning for variable-resolution isosurfaces. In: Computer Graphics International, Tokyo, June 1992. pp. 22–6.
[9] Shekhar R, Fayyad E, Yagel R, Cornhill JF. Octree-based decimation of marching cubes surfaces. IEEE Visualization, 1996. pp. 335–449.
[10] Oh KM, Park KH. A vertex merging algorithm for extracting a

variable-resolution isosurface from volume data. IEEE International Conference on System Man and Cybernetics, Vol. 4, 1995. pp. 3543–8.
[11] Baker HH. Building surfaces of evolution: the weaving wall. Int J Computer Vision 1989;3:51–71.
[12] Cline HE, Lorensen WE, Ludke S, Crawford CR, Teeter BC. Two algorithms for the three-dimensional reconstruction of tomograms. Med Phys 1988;15:320–7.
[13] Durst MJ. Additional reference to marching cubes. Computer Graph 1988;22:72–73.
[14] Nielson GM, Hamann B. The asymptotic decider: resolving the ambiguity in marching cubes. In: Proceedings of Visualization 1991 Conference, San Diego, CA, 1991. pp. 83–91.
[15] Li J, Agathoklis P. An efficiency enhanced isosurface generation algorithm for volume visualization. The Visual Computer 1997;13:391–400.
[16] Wilhelms J, Van Gelder A. Octree for faster isosurface generation. ACM Trans Graph 1992;11:201–27.
[17] C. Montani, R. Scateni, R, Scopigno. Discretized Marching Cubes. IEEE Conference on Visualization, 1994. pp. 281–7.
[18] Manocha D, Narkhede A. Fast polygon triangulation based on Seidel's algorithm, 1995. http://www.cs.unc.edu/~dm/CODE/GEM/chapter.html.
[19] Seidel R. A simple and fast incremental randomized algorithm for computing trapezoidal decompositions and triangulating polygons, computational geometry: theory and applications, 1991. pp. 51–64.
[20] Bajaj et al. Fast isocontouring for improved interactivity. In: Proceedings of 1996 Symposium on Vol. Vis., San Francisco, October 1996.
[21] Westermann, et al. Real-time exploration of regular volume data by adaptive reconstruction of isosurfaces. The Visual Computer 1999;15:110–1.
[22] Nielson GM, Hamann B. The asymptotic decider: resolving the ambiguity in marching cubes. In: IEEE Conference Visualization 1991. pp. 83–91.

Tong-Yee Lee was born in Tainan county, Taiwan, Republic of China, in 1966. He received his BS in Computer Engineering from Tatung Institute of Technology in Taipei, Taiwan, in 1988, his MS in Computer Engineering from National Taiwan University in 1990, and his PhD in Computer Engineering from Washington State University, Pullman, in May 1995. Now, he is an Associate Professor in the Department of Computer Science and Information Engineering at National Cheng-Kung University in Tainan, Taiwan, Republic of China. He was with WSU as a Visiting Research Professor at School of EE/CS during 1996 summer and serves as guest associated editor for *IEEE Transactions on Information Technology in Biomedicine* in 2000. He has been working on parallel rendering and computer graphics since 1992, and has published more than 65 technical papers in referred journals and conferences. His current research interests include computer graphics, medical visualization, virtual reality, surgical simulation, distributed and collaborative virtual environment, parallel processing and heterogeneous computing.

Chao-Hung Lin was born in Koushung, Taiwan, Republic of China, in 1973. He received his BS in Computer Science/Engineering from Fu-Jen University and MS in Computer Engineering from National Cheng-Kung University, Taiwan, Republic of China, in 1997 and 1998, respectively. Now, he is pursuing his PhD degree at Department of Computer Science and Information Engineering, National Cheng-Kung University. Mr Lin research interests include computer graphics, image processing, virtual reality, visualization and interactive rendering.